THE JOURNAL OF BIOLOGICAL CHEMISTRY
Vol. 272, No. 28, Issue of July 11, pp. 17349–17353, 1997
Printed in U.S.A.
© 1997 by The American Society for Biochemistry and Molecular Biology, Inc.

The Ferrous-dioxy Complex of Neuronal Nitric Oxide Synthase

DIVERGENT EFFECTS OF L-ARGININE AND TETRAHYDROBIOPTERIN ON ITS STABILITY*

(Received for publication, March 14, 1997, and in revised form, May 2, 1997)

Husam M. Abu-Soud‡§, Ratan Gachhui‡, Frank M. Raushel¶, and Dennis J. Stuehr‡§‖

From the ‡Department of Immunology, The Cleveland Clinic Research Institute, Cleveland, Ohio 44195 and ¶Department of Chemistry, Texas A&M University, College Station, Texas 77843

Nitric oxide synthases (NOS) are hemeproteins that catalyze oxidation of L-arginine to nitric oxide (NO) and citrulline. The NOS heme iron is expected to participate in oxygen activation during catalysis, but its interactions with O_2 are not characterized. We utilized the heme-containing oxygenase domain of neuronal NOS (nNOSoxy) and stopped-flow methods to study formation and autooxidative decomposition of the nNOSoxy oxygenated complex at 10 °C. Mixing ferrous nNOSoxy with air-saturated buffer generated a transient species with absorption maxima at 427 and ~560 nm. This species decayed within 1 s to form ferric nNOSoxy. Its formation was first order with respect to O_2, monophasic, and gave rate constants for $k_{on} = 9 \times 10^5\ M^{-1}\ s^{-1}$ and $k_{off} = 108\ s^{-1}$ for an L-arginine- and tetrahydrobiopterin (H_4B)-saturated nNOSoxy. Omission of L-arginine and/or H_4B did not greatly effect O_2 binding and dissociation rates. Decomposition of the oxygenated intermediate was independent of O_2 concentration and was either biphasic or monophasic depending on sample conditions. L-Arginine stabilized the oxygenated intermediate (decay rate = $0.14\ s^{-1}$), while H_4B accelerated its decay by a factor of 70 irrespective of L-arginine. The spectral and kinetic properties of the intermediate identify it as the $Fe^{II}O_2$ complex of nNOSoxy. Destabilization of a metallo-oxy species by H_4B is unprecedented and may be important regarding the role of this cofactor in NO synthesis.

Nitric oxide (NO)[1] is an ubiquitous signal molecule involved in the regulation of several activities in the cardiovascular, nervous, and immune systems (1–4). NO is generated by a family of enzymes termed NO synthases (NOSs), which catalyze an NADPH- and O_2-dependent two-step oxidation of L-arginine to form NO and citrulline (5, 6). All NOSs are comprised of a C-terminal reductase domain that contains the binding sites for calmodulin (CaM), FMN, FAD, and NADPH and an N-terminal oxygenase domain that contains binding sites for iron protoporphyrin IX (heme), tetrahydrobiopterin (H_4B), and substrate (L-arginine) (7–13). A variety of evidence suggests the individual oxygenase and reductase domains can fold and function independently (8–10, 13, 14). The neuronal NOS isoform (nNOS) is constitutively expressed in an inactive form that requires Ca^{2+}-dependent CaM binding to activate its NO synthesis (15, 16). CaM activates NO synthesis in part by triggering an interdomain electron transfer between the flavin and heme centers of nNOS (17, 18).

The NOS heme iron is axially coordinated to the protein via a cysteine thiolate, as is the case for cytochrome P450s, and is predominantly five-coordinate and high spin in its ferric state (19–21). Substrate appears to bind directly above the heme and can interact with ligands bound to the heme iron, such as CO or NO (22, 23). During catalysis of NO synthesis, such positioning may alter heme iron reactivity or sterically specify substrate hydroxylation events as catalyzed by the heme iron. The H_4B cofactor is critical for stabilizing NOS dimeric structure and maintaining catalytic activity (24–26), and also affects the heme iron spin state, axial ligand stability, and binding of exogenous ligands (9, 27–29).

Reduction of the NOS heme iron is associated with activation of NO synthesis from L-arginine or with production of superoxide and H_2O_2 in the absence of substrate (17, 27, 30, 31). Heme iron reduction is thought to be critical for both activities because it may enable the enzyme to bind and activate O_2 (5, 6). Indeed, NO synthesis from either L-arginine or the reaction intermediate N^{ω}-hydroxyarginine is diminished in the presence of ligands that may prevent O_2 binding to the heme iron, such as CO or imidazole (32, 33). Although complexes between the NOS heme iron and CO, NO, and CN^- have been characterized spectroscopically (19–23, 34), direct evidence of O_2 binding to the NOS ferrous heme iron is not available.

To investigate what role the NOS heme plays in oxygen activation during catalysis, we utilized the oxygenase domain of nNOS[2] (nNOSoxy, amino acids 1–720) to study reactions between its ferrous heme iron and O_2. This report provides direct evidence for formation of a transient NOS $Fe^{II}O_2$ complex, and characterizes how bound L-arginine and H_4B effect its formation and decay kinetics.

EXPERIMENTAL PROCEDURES

Materials—Oxygen gas was purchased from Liquid Carbonic Company. All other reagents and materials were obtained from Sigma or from sources reported previously (14, 24, 30).

Protein Expression and Purification—Rat nNOS cDNA was a gift from Drs. David Bredt and Solomon Snyder at the John Hopkins University. The pCWori plasmid was used to overexpress the nNOSoxy (amino acids 1–723 with a six-histidine tag incorporated at the C terminus) in *Escherichia coli* strain BL21(DE3). The procedure to incorporate nNOSoxy cDNA into the pCWori plasmid was similar to that

* This study was supported by National Institute of Health Grant GM51491 (to D. J. S). The costs of publication of this article were defrayed in part by the payment of page charges. This article must therefore be hereby marked "*advertisement*" in accordance with 18 U.S.C. Section 1734 solely to indicate this fact.

§ To whom correspondence should be addressed: Immunology NN-1, Cleveland Clinic, 9500 Euclid Ave., Cleveland, OH 44195. Tel.: 216-445-6950; Fax: 216-444-9329.

‖ Established Investigator of the American Heart Association.

[1] The abbreviations used are: NO, nitric oxide; nNOS, neuronal nitric oxide synthase; nNOSoxy, the oxygenase domain of nNOS; CaM, calmodulin; H_4B, (6*R*,6*S*)-2-amino-4-hydroxy-6-(L-erythro-1,2-dihydroxypropyl)-5,6,7,8-tetrahydropteridine; PCR, polymerase chain reaction; PMSF, phenylmethylsulfonyl fluoride; EPPS, 4-(2-hydroxyethyl)-1-piperazinepropanesulfonic acid; Bis-Tris, 2-[bis(2-hydroxyethyl)-amino]-2-(hydroxymethyl)-propane-1,3-diol.

[2] Use of nNOSoxy eliminates spectral interference from bound flavin groups present in the full-length enzyme.

Downloaded from http://www.jbc.org/ at Texas A&M University Libraries on April 21, 2015

reported by McMillan and Masters (9). PCR was used to amplify the nNOSoxy DNA (corresponding to amino acids 1–720 with an incorporated hexahistidine tag at the C terminus), using as a template a pCIS-2 construct of full-length nNOS. The oligonucleotides used were 5′-ATATTGACCATATGGAAGAGAACACGTTTGGG as the forward primer (to create an *Nde*I site), and 5′-ATATTGACGTCGACTTAGTG-GTGGTGGTGGTGGTGGTTGGTGCCCTTCCACACG as the backward primer (to create the hexahistidine tag and a stop codon followed by an *Sal*I site). PCR was done using the Expand Long Template system from Boehringer Mannheim. A typical 50-μl mixture included 350 μM dNTPs, 100 pmol of each primer, 10 ng of nNOS template, PCR buffer containing 1.75 mM $MgCl_2$, and 2.5 units of enzyme mix containing *Taq* and *Pwo* DNA polymerases. The PCR product was restricted with *Nde*I and *Sal*I and ligated into a similarly restricted pCWori plasmid. The product was transformed to competent *E. coli* BL21(DE3) cells and transformants were selected on LB plates containing 125 mg/L ampicillin. The sequence of the final construct was checked at the DNA core facility of the Cleveland Clinic Foundation.

One liter of Terrific Broth (Life Technologies, Inc.) containing 4 ml of glycerol and 125 mg of ampicillin was inoculated with a 50-ml overnight culture of the bacteria containing the plasmid for expression of nNOSoxy and grown at 37 °C at 250 rpm up to an A_{600} of 1. Protein expression was then induced by adding 1 mM isopropyl-1-thio-β-D-galactopyranoside along with 0.4 mM δ-aminolevulinic acid, and the culture was grown at 25 °C for 2 days. Cells were harvested and suspended in the buffer A (40 mM EPPS, pH 7.6, 10% glycerol, 0.25 M NaCl) containing protease inhibitors and 1 mg/ml lysozyme, lysed by three cycles of freeze-thawing, and sonicated (three times at 30 s each with a 1-min rest on ice between the pulses). Cell-free supernatant obtained after centrifugation at 30,000 × *g* for 30 min at 4 °C was applied to a column containing Ni^{2+}-nitrilotriacetic acid resin (10 ml) equilibrated with buffer A containing 1 mM PMSF. The column was washed with 100 ml of buffer A containing 1 mM PMSF and then eluted with buffer A containing 40 mM imidazole and 1 mM PMSF, and 1.5-ml fractions were collected. Fractions containing nNOSoxy were pooled and concentrated using a Centriprep-30. The protein was dialyzed against buffer A without NaCl and containing 1 mM dithiothreitol and stored in aliquots at −70 °C. The purity of the protein was estimated to be 90% as judged by SDS-polyacrylamide gel electrophoresis. The hemeprotein concentration was estimated based on the absorbance at 444 nm for the ferrous-CO complex, using an extinction coefficient 76 mM^{-1} cm^{-1} (21).

Sample and Solution Preparation—The nNOSoxy samples were dialyzed overnight at 4 °C against 40 mM Bis-Tris propane, pH 7.4, containing 1 mM dithiothreitol alone or plus 4 μM H_4B, plus 3 mM L-arginine, or plus H_4B and L-arginine. L-Arginine and H_4B saturation of nNOSoxy samples was confirmed spectroscopically (35). The protein solutions were made anaerobic by repeated cycles of evacuation and equilibration with catalyst-deoxygenated N_2 before use in stopped-flow experiments.

Solutions of 40 mM Bis-Tris propane, pH 7.4, containing various concentrations of O_2 were prepared by mixing different volumes of O_2-saturated buffer with air-saturated or anaerobic buffer solutions. Saturation was achieved by bubbling O_2 for 2 h in a septum-sealed flask at 21 °C. Final O_2 concentrations were calculated based on a saturating O_2 concentration of 1.2 mM at 21 °C.

Optical Spectroscopy—Anaerobic spectra of ferrous nNOSoxy were recorded at 15 °C in septum-sealed quartz cuvettes that could be attached through a ground-glass joint to a vacuum gas train.

Rapid Kinetic Measurements—Measurements were obtained using a stopped-flow apparatus from Hi-tech Ltd. (model SF-51) equipped for anaerobic work. Measurements were carried out at 10 °C and initiated by mixing anaerobic solutions of 5 μM nNOSoxy that had been prereduced with excess dithionite (40 μM) with an equal volume of buffer containing O_2 at different concentrations. Formation and decay of the oxygenated nNOSoxy complex were monitored at 410 nm, 405 nm, or at other wavelengths as indicated in the text. In some experiments, the stopped-flow instrument was equipped with a rapid-scanning detector (Hi-Tech, MG-3000) designed to collect a complete spectrum (200–800 nm) within 90 ms. The detector was calibrated relative to four principal peak absorption wavelengths of a didymium filter (BG 20) at 236, 358, 584, and 738 nm. Rapid scanning involved mixing anaerobic solutions containing 6 μM dithionite-reduced nNOSoxy, 2 mM L-arginine, and 10 μM H_4B with air-saturated buffer at 6 °C. In all cases, 10–20 successive scans were recorded to generate an average.

The time course of oxygenated complex formation and decay were fit to Equations 1 and 2 by use of a nonlinear least-squares method provided by the instrument manufacturer, where

$$Y = Ae^{-k_1 t} + C \quad \text{(Eq. 1)}$$

$$Y = Ae^{-k_1 t} + Be^{-k_2 t} + C \quad \text{(Eq. 2)}$$

k_1 and k_2 are first-order rate constants, *t* is time, *A* and *B* are amplitude factors, *e* is 2.718, and *C* is a constant. Equation 1 describes a process that takes place via single exponential decay, while Equation 2 represents the sum of two independent exponentials for a parallel process.

FIG. 1. **Formation of the ferrous nNOSoxy-dioxygen complex.** The *upper panel* shows the rapid scanning spectra for the intermediate and final products formed by reacting ferrous nNOSoxy with air-saturated buffer in the presence of saturating L-arginine and H_4B. The first spectrum (*dashed line*, $Fe^{2+}O_2$) was collected within 7 ms of initiating the reaction while the second spectrum (*solid line*, Fe^{3+}) was collected 25 s after mixing. Intermediate spectra were omitted for clarity. The *lower panel* shows the absorbance spectra of the nNOSoxy ferric (*solid line*, Fe^{3+}) and deoxyferrous (*dotted line*, Fe^{2+}) forms in the presence of saturating H_4B and L-arginine.

RESULTS

Rapid mixing a solution of ferrous nNOSoxy containing L-arginine and H_4B with an equal volume of air-saturated buffer resulted in formation of a transient species whose spectrum was characterized by absorbance peaks at 427 and ~560 nm (Fig. 1, *upper panel*). This spectrum differs from that of either ferric or ferrous nNOS, whose Soret maxima are centered at 400 nm or 414 nm, respectively (Fig. 1, *lower panel*), but is similar to that of $Fe^{II}O_2$ cytochrome P-450s, whose Soret maxima range from 418 to 423 nm (36–44). A similar species was observed when reacting ferrous nNOSoxy with O_2 in the absence of L-arginine and H_4B, indicating that these molecules are not required for generating the transient species. The nNOSoxy intermediate formed within 7 ms after mixing at 10 °C, but was unstable and converted to its ferric form within 1 s as judged by a time-dependent shift in Soret absorbance from 427 to 400 nm (Fig. 1, *upper panel*). Thus, formation of the nNOSoxy intermediate and its subsequent autooxidation occur at sufficiently different rates to enable each process to be studied by conventional stopped-flow methods.

To investigate more closely the formation and decay of the oxygenated intermediate, we monitored absorbance change at various single wavelengths. Traces obtained at 410 or 440 nm are shown in Fig. 2. Changes in absorbance *versus* time were biphasic at both wavelengths. For the reaction monitored at 410 nm (*upper panel*), there was a rapid initial absorbance decrease fol-

Downloaded from http://www.jbc.org/ at Texas A&M University Libraries on April 21, 2015

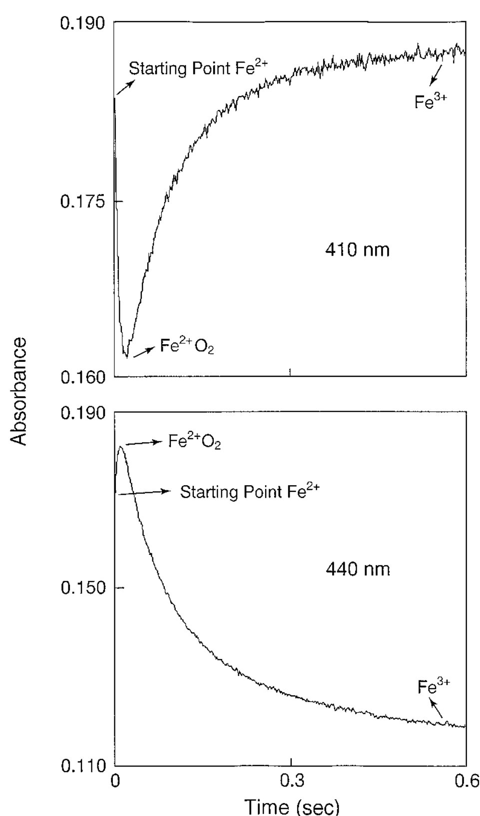

FIG. 2. **Stopped-flow traces for the reaction of ferrous nNOSoxy with air-saturated buffer.** The reaction was monitored at 410 nm (*upper panel*) and 440 nm (*lower panel*) in the presence of saturating L-arginine and H_4B. Points that are associated with maximum absorbance of individual nNOSoxy species are indicated in each panel.

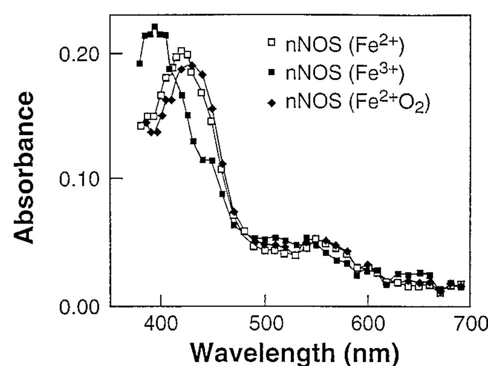

FIG. 3. **Spectra of the ferric, ferrous, and oxygenated nNOSoxy species derived from single wavelength stopped-flow analysis.** Ferrous nNOSoxy was rapid-mixed with air-saturated buffer in the presence of saturating L-arginine and H_4B. Stopped-flow traces were obtained at the single wavelengths indicated by the position of each symbol. The maximum absorbance due to each of the three nNOS species was obtained from the kinetic traces at each wavelength (as exemplified in Fig. 2) and used to construct a spectrum for each species.

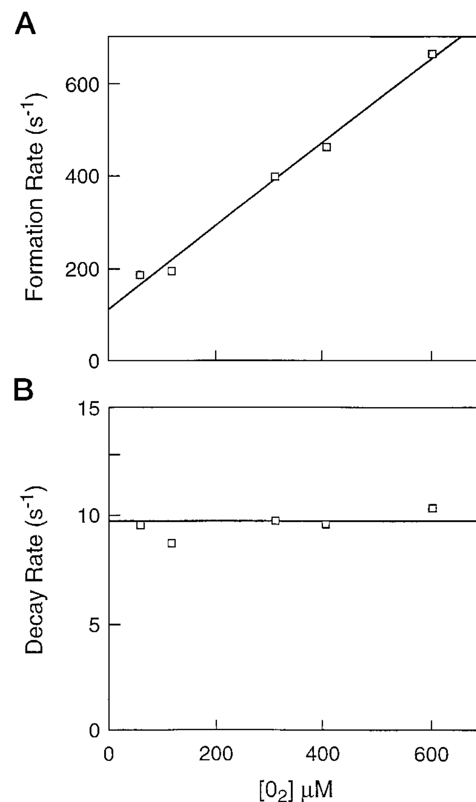

FIG. 4. **Effect of O_2 concentration on the formation and decay of the oxygenated nNOSoxy complex.** A solution of 2 μM ferrous nNOSoxy containing 1 mM L-arginine and 10 μM H_4B was rapid-mixed at 10 °C with buffer containing different O_2 concentrations. *Panel A* plots the observed rates of complex formation at 410 nm *versus* O_2 concentration, while *panel B* plots the observed decay rates of the oxygenated nNOSoxy complex at 410 nm *versus* O_2 concentration.

lowed by a slower increase in absorbance. When the reaction was monitored at 440 nm (*lower panel*), the direction of absorbance change was reversed but otherwise proceeded with identical kinetics. At either wavelength, the absorbance observed at the start of the reaction can be attributed to ferrous nNOSoxy, while the absorbance at the inflection and end points can be attributed to sequential formation of the transient intermediate and ferric nNOSoxy, respectively. We thus monitored the reaction at a range of single wavelengths and plotted the maximum absorbance obtained for each of the three species as a function of wavelength. As shown in Fig. 3, the spectra so derived match the rapid scanning spectra reported in Fig. 1 and are consistent with the sequential nature of the proposed reaction. Fitting each stopped-flow trace obtained at single wavelengths to a two-exponential function showed that there was no variation in the observed rate constants for formation or autooxidation. This indicates that the transient intermediate and ferric nNOSoxy are the only two observable products of the reaction.

We next examined the formation and decay of the transient species as a function of O_2 concentration by monitoring absorbance change at 410 nm. The pseudo-first order rate constants obtained for its formation in the presence of saturating L-arginine and H_4B are plotted as a function of O_2 concentration in *panel A* of Fig. 4. The association and dissociation rate constants derived from the graph are listed in Table I along with rate constants obtained under similar conditions for nNOSoxy samples saturated either with L-arginine or H_4B alone or in the absence of both molecules.

As shown in *panel B* of Fig. 4, the decay rate of the transient species did not change with O_2 concentration, indicating decay is independent of dissolved O_2. The autooxidation rate for the H_4B- and L-arginine-saturated protein was best fit to a single exponential function and was therefore monophasic, giving a rate of 10 s^{-1} (Table I). An identical monophasic decay rate was also observed with nNOSoxy that was saturated with H_4B alone (Table I). However, decay of the transient species in nNOSoxy samples devoid of both L-arginine and H_4B was biphasic, giving rate constants of 2.3 s^{-1} and 0.12 s^{-1} (Table I). Again, these decay rates did not change as a function of O_2 concentration (data not shown). With an nNOS sample satu-

Downloaded from http://www.jbc.org/ at Texas A&M University Libraries on April 21, 2015

TABLE I
Rate constants for formation and decay of the oxygenated nNOSoxy complex

Ferrous nNOSoxy in the presence or absence of L-arginine and/or H_4B was rapid-mixed with buffer containing O_2 at various concentrations. Rates of complex formation and decay were determined by following absorbance change at 410 nm, and the rate constants determined as described in the text.

Conditions	k_{on}	k_{off}	Decay
	$M^{-1}s^{-1}$	s^{-1}	
−L-Arginine − H_4B	1.4×10^6	177	0.12, 2.3
+L-Arginine − H_4B	1.1×10^6	65	0.14
−L-Arginine + H_4B	7.8×10^5	130	10
+L-Arginine + H_4B	9.0×10^5	108	10

rated with L-arginine alone, only the slow decay rate was observed (Table I).

DISCUSSION

These data provide the first direct evidence for O_2 binding to the NOS heme iron, consistent with its proposed role in oxygen activation during NO synthesis (5, 6). Mixing an O_2-containing solution with ferrous nNOSoxy resulted in rapid formation of a transient intermediate whose spectral and kinetic characteristics were quite similar to the $Fe^{II}O_2$ complexes of a number of cytochrome P-450s (36–44), identifying the intermediate as $Fe^{II}O_2$ nNOSoxy. Although its Soret maxima (427 nm) is somewhat red-shifted compared with most $Fe^{II}O_2$ cytochrome P-450s which absorb maximally at 418–420 nm (36–40, 42–44), it is most similar to the $Fe^{II}O_2$ complex of substrate-bound cytochrome P-450$_{SCC}$ which absorbs maximally at 423 nm (41). The spectral features of $Fe^{II}O_2$ nNOSoxy did not change noticeably in the absence of bound substrate (L-arginine) or H_4B (data not shown), consistent with bound substrate also not altering the visible spectra of the ferrous-CO or -NO complexes of nNOS (19, 23, 30).

In air-saturated solution, formation of the nNOSoxy $Fe^{II}O_2$ complex occurred at a rates that were 40–4000 times faster than complex decay. Under such circumstances, practically all of the nNOSoxy sample exists in its $Fe^{II}O_2$ form prior to decay.[3] Rates of complex formation and decay were invariant as a function of wavelength and both processes generated spectral isosbestic points. This indicates that complex formation and decay occur without formation of other observable intermediates, which is also the case for most cytochrome P450s examined to date (36, 40). Formation of $Fe^{II}O_2$ nNOSoxy was first order with respect to O_2, reversible, and followed a simple one-step mechanism. Decay of the complex was independent of O_2 concentration, occurred via a one- or two-exponential process depending on sample conditions, and generated ferric nNOSoxy as a product. A model consistent with the data is shown in Scheme 1. Mechanisms proposed for the autooxidation of $Fe^{II}O_2$ hemeproteins generally involve electron transfer to O_2 as a primary step to form superoxide, which undergoes further irreversible reactions (45, 46). Indeed, uncoupled NADPH oxidation by nNOS is reported to generate superoxide as a primary product (31). However, because cytochrome P-450s can also generate H_2O_2 or water as primary products of uncoupled oxidation (36, 47, 48), it is possible that nNOS may form these products under favorable conditions.

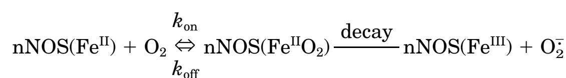

SCHEME 1

Dioxygen binding to ferrous nNOSoxy was fast enough to be kinetically competent regarding NO synthesis (5, 6), and the second order rate constants were comparable to that published for ferrous cytochrome P-450$_{CAM}$ (40). However, estimated rate constants for O_2 dissociation from ferrous nNOSoxy were one to two orders of magnitude greater than that published for P-450$_{CAM}$ (40). The reason for this difference is unclear. L-arginine or H_4B did not significantly influence O_2 binding and dissociation rates, suggesting that the O_2 interaction is not greatly influenced by bound substrate or pterin. This differs from CO, whose rebinding to the nNOS heme is decreased 12-fold in the presence of bound L-arginine (34). We speculate this difference may arise from steric constraints in the distal pocket brought on by substrate and pterin that appear to force a bent Fe^{II}-ligand geometry (22, 23) instead of the linear geometry particularly favored by ferrous-CO complexes.

In the absence of L-arginine and H_4B, the autooxidation of $Fe^{II}O_2$ nNOSoxy was biphasic, giving rate constants of 0.12 and 2.3 s^{-1}. Only the slow decay rate was observed in the presence of L-arginine, implying that bound substrate stabilizes $Fe^{II}O_2$ nNOSoxy. Biphasic decay in the absence of substrate and/or stabilization in its presence have also been reported for some $Fe^{II}O_2$ cytochrome P-450s (36, 41, 44). However, even in its most stable form (*i.e.* L-arginine-bound) the $Fe^{II}O_2$ nNOSoxy complex still decays 2 or 100 times faster than the substrate-bound $Fe^{II}O_2$ complexes of cytochrome P-450$_{SCC}$ (41) and P-450$_{CAM}$ (40), respectively.

Remarkably, bound H_4B accelerated the decay of $Fe^{II}O_2$ nNOS by a factor of 70 even in the presence of bound L-arginine. The apparent ability of H_4B to destabilize an oxy-iron complex is unprecedented and represents a new role for pterins in biology. The impact of this finding on NOS catalysis is not yet clear. However, it is pertinent to discuss with regard to oxygen activation during NO synthesis, which is thought to proceed as in the cytochrome P-450s (reviewed in Ref. 49) (Scheme 2).

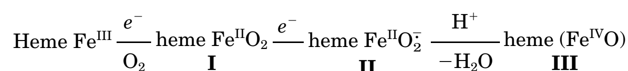

SCHEME 2

Initial reduction of the ferric heme iron enables formation of the $Fe^{II}O_2$ species (**I**). Transfer of a second electron is thought to generate an iron-peroxy intermediate (**II**) that loses water and forms a high valence oxo-iron species (**III**) that can carry out substrate hydroxylation.

In NOS, the $Fe^{II}O_2$ species (**I**) has been proposed to play a different role in each step of catalysis (5, 6). In the first step (*N*-hydroxylation of L-arginine) it may function solely as an intermediate on the path to the oxo-iron species (**III**) that is thought to hydroxylate L-arginine. However, in the second step (conversion of the *N*-hydroxyarginine intermediate to NO and citrulline) the $Fe^{II}O_2$ species (**I**) may instead act as an oxidant that removes an electron or hydrogen atom from bound *N*-hydroxyarginine.[4] Thus, productive oxygen activation in both

[3] This enabled us to estimate an extinction coefficient for the nNOSoxy $Fe^{II}O_2$ complex (64.1 $mM^{-1}\ cm^{-1}$ at 427 nm), which is lower than the estimated extinction coefficients of ferric or ferrous nNOSoxy (76 and 69.1 $mM^{-1}\ cm^{-1}$ at 400 and 414 nm, respectively).

[4] An investigation of nNOS catalysis under single turnover conditions shows that the $Fe^{II}O_2$ species can catalyze the second step of NO synthesis, consistent with its acting as an oxidant in this step (H. M. Abu-Soud, P. A. Presta, B., Mayer, and D. J. Stuehr, unpublished results).

Downloaded from http://www.jbc.org/ at Texas A&M University Libraries on April 21, 2015

steps of NO synthesis may require that a second electron be provided to the Fe^{II}O$_2$ complex. When viewed this way, destabilization of the Fe^{II}O$_2$ complex by H$_4$B seems counterproductive, because it would favor a decomposition reaction that yields ferric nNOS and superoxide instead of further reductive steps that lead to NO synthesis. However, the fact that NO synthesis by nNOS is tightly coupled to NADPH oxidation in the presence of saturating H$_4$B (5, 6) suggests that decay of the Fe^{II}O$_2$ species under normal reaction conditions is slower than the additional reductive steps required to activate oxygen for productive catalysis.

Recent work with H$_4$B-free forms of nNOS (27) and inducible NOS[5] shows that they can catalyze NADPH-dependent, heme iron-based O$_2$ consumption in the presence of bound L-arginine without catalyzing NO synthesis. This implies that formation of oxygenated iron species within the active site can occur in the absence of H$_4$B but is itself not sufficient to support NO synthesis. Thus, we speculate that H$_4$B destabilization of the nNOSoxy Fe^{II}O$_2$ complex as described here may actually reflect a more global influence of H$_4$B on the reactivity of all nNOS iron-oxy species that somehow enables oxygen activation at the heme to become coupled to NO synthesis. Our current findings provide a foundation to explore this hypothesis.

Acknowledgments—We thank Pam Clark, Jingli Zhang, Bryant Miles, and Suk-Bong Hong for excellent technical assistance.

REFERENCES

1. Ignarro, L. J. (1990) *Annu. Rev. Pharmacol. Toxicol.* **30,** 535–560
2. Moncada, S., Palmer, R. M. J., and Higgs, E. A. (1991) *Pharmacol. Rev.* **43,** 109–142
3. Schmidt, H. H. H. W., and Walter, U. (1994) *Cell* **78**, 919–925
4. Vincent, S. R. (1994) *Prog. Neurobiol.* **42,** 129–160
5. Marletta, M. A. (1993) *J. Biol. Chem.* **268,** 12231–12234
6. Griffith, O. W., and Stuehr, D. J. (1995) *Annu. Rev. Physiol.* **57,** 707–736
7. Bredt, D. S., Hwang, P. M., Glatt, C. E., Lowenstein, C., Reed, R. R., and Snyder, S. H. (1991) *Nature* **351,** 714–718
8. Sheta, E. A., McMillan, K., and Masters, B. S. S.(1994) *J. Biol. Chem.* **269,** 15147–15153
9. McMillan, K., and Masters, B. S. S. (1995) *Biochemistry* **34,** 3686–3693
10. Ghosh, D. K., Abu-Soud H. M., and Stuehr D. J. (1996) *Biochemistry* **35,** 1444–1449
11. Klatt, P., Schmidt, K., Brunner, F., and Mayer, B. (1994) *J. Biol. Chem.* **269,** 1674–1680
12. Ghosh, D. K., and Stuehr, D. J. (1995) *Biochemistry* **34,** 801–807
13. Chen, P.-F., Tsai, A.-L., Berka, V., and Wu, K. K. (1996) *J. Biol. Chem.* **271,** 14631–14635
14. Gachhui, R., Presta, A., Bentley, D. F., Abu-Soud, H. M., McArthur, R., Brudvig, G., Ghosh, D. K., and Stuehr, D. J. (1996) *J. Biol. Chem.* **271,** 20594–20602

[5] P. A. Presta, U. Siddhanta, and D. J. Stuehr, unpublished results.

15. Nakane, M., Schmidt, H. H. H. W., Pollock, J. S., Forstermann, U., and Murad, F. (1993) *FEBS Lett.* **316,** 175–180
16. Su, Z., Blazing, M. A., Fan, D., and George, S. E. (1995) *J. Biol. Chem.* **270,** 29117–29122
17. Abu-Soud, H. M., and Stuehr, D. J. (1993) *Proc. Natl. Acad. Sci. U. S. A.* **90,** 10769–10772
18. Abu-Soud, H. M., Yoho, L. L., and Stuehr, D. J. (1994) *J. Biol. Chem.* **269,** 32047–32050
19. McMillan, K., Bredt, D. S., Hirsch, D. J., Snyder, S. H., Clark, J. E., and Masters, B. S. S. (1992) *Proc. Natl. Acad. Sci. U. S. A.* **89,** 11141–11145
20. Sono, M., Stuehr, D. J., Ikeda-Saito, M., and Dawson, J. H. (1995) *J. Biol. Chem.* **270,** 19943–19948
21. Stuehr, D. J., and Ikeda-Saito, M. (1992) *J. Biol. Chem.* **267,** 20547–20550
22. Wang, J., Stuehr, D. J., Ikeda-Saito, M., and Rousseau, D. L. (1993) *J. Biol. Chem.* **268,** 22255–22258
23. Wang, J., Rousseau, D. L., Abu-Soud, H. M., and Stuehr, D. J. (1994) *Proc. Natl. Acad. Sci. U. S. A.* **91,** 10512–10516
24. Baek, K. J., Thiel, B. A., Lucas, S., and Stuehr, D. J. (1993) *J. Biol. Chem.* **268,** 21120–21129
25. Klatt, P., Schmidt, K., Lehner, D., Glatter, O., Bachinger, H. P., and Mayer, B. (1995) *EMBO J.* **14,** 3687–3695
26. Hevel, J. M., and Marletta, M. A. (1992) *Biochemistry* **31,** 7160–7165
27. Gorren, A. C. F., List, B. M., Schrammel, A., Pitters, E., Hemmens, B., Werner, E. R., Schmidt, K., and Mayer, B. (1996) *Biochemistry* **35,** 16735–16745
28. Wang, J., Stuehr, D. J., and Rousseau, D. L. (1995) *Biochemistry* **34,** 7080–7087
29. Rodriguez-Crespo, I., Gerber, N. C., and Ortiz de Montellano, P. R. (1996) *J. Biol. Chem.* **271,** 11462–11467
30. Abu-Soud, H. M., Feldman, P. L., Clark, P., and Stuehr, D. J. (1994) *J. Biol. Chem.* **269,** 32318–32326
31. Pou, S., Pou, W. S., Bredt, D. S., Snyder, S. H., and Rosen, G. M. (1992)*J. Biol. Chem.* **267**, 24173–24176
32. Pufahl, R. A., and Marletta, M. A. (1993) *Biochem. Biophys. Res. Commun.* **193,** 963–970
33. Wolff, D. J., Datto, G. A., Samatovicz, R. A., and Tempsick, R. A. (1993) *J. Biol. Chem.* **268,** 9425–9429
34. Matsuoka, A., Stuehr, D. J., Olson, J. S., Clark, P., and Ikeda-Saito, M. (1994) *J. Biol. Chem.* **269,** 20335–20339
35. Abu-Soud, H. M., Loftus, M., and Stuehr, D. J. (1995) *Biochemistry* **34,** 11167–11175
36. Oprian D. D., Gorsky L. D., and Coon M. J. (1983) *J. Biol. Chem.* **258,** 8684–8691
37. Guengerich, F. P., Ballou, D. P., and Coon, M. J. (1976) *Biochem. Biophys. Res. Commun.* **70,** 951–956
38. Tyson, C. A., Lipscomb, J. D., and Gunsalus, I. C. (1972) *J. Biol. Chem.* **247,** 5777–5784
39. Ishimura, Y., Ullrich, V., and Peterson, J. A. (1971) *Biochem. Biophys. Res. Commun.* **42,** 140–146
40. Peterson, J. A., Ishimura, Y., and Griffin, B. W. (1972) *Arch. Biochem. Biophys.* **149,** 197–208
41. Tuckey, R. C., and Kamin, H. (1982) *J. Biol. Chem.* **257,** 9309–9314
42. Larroque, C., and Van Lier, J. E. (1980) *FEBS Lett.* **115,** 175–177
43. Eisenstein, L., Debey, P., and Douzou, P. (1977) *Biochem. Biophys. Res. Commun.* **77,** 1377–1283
44. Bonfils, C., Debey, P., and Maurel, P. (1979) *Biochem. Biophys. Res. Commun.* **88,** 1301–1307
45. Momenteau M., and Reed C. A. (1994) *Chem. Rev.* **94,** 659–698
46. Sligar, S. G., Lipscomb, J. D., Debrunner, P. G., and Gunsalus, I. C. (1974) *Biochem. Biophys. Res. Commun.* **61,** 290–296
47. Loida, P. J., and Sligar, S. G. (1993) *Biochemistry* **32,** 11530–11538
48. Gorsky, L. D., Koop, D. R., and Coon, M. J. (1984) *J. Biol. Chem.* **259,** 6812–6817
49. Guengerich, F. P., and Macdonald, T. L. (1990) *FASEB J.* **4,** 2453–2459

Downloaded from http://www.jbc.org/ at Texas A&M University Libraries on April 21, 2015

The Journal of Biological Chemistry
AFFINITY SITES
ASBMB
American Society for Biochemistry and Molecular Biology

ENZYMOLOGY:

The Ferrous-dioxy Complex of Neuronal Nitric Oxide Synthase: DIVERGENT EFFECTS OF l-ARGININE AND TETRAHYDROBIOPTERIN ON ITS STABILITY

Husam M. Abu-Soud, Ratan Gachhui, Frank M. Raushel and Dennis J. Stuehr

J. Biol. Chem. 1997, 272:17349-17353.
doi: 10.1074/jbc.272.28.17349

Access the most updated version of this article at http://www.jbc.org/content/272/28/17349

Find articles, minireviews, Reflections and Classics on similar topics on the JBC Affinity Sites.

Alerts:
- When this article is cited
- When a correction for this article is posted

Click here to choose from all of JBC's e-mail alerts

This article cites 49 references, 24 of which can be accessed free at
http://www.jbc.org/content/272/28/17349.full.html#ref-list-1

Downloaded from http://www.jbc.org/ at Texas A&M University Libraries on April 21, 2015